Research Article

Effect of intensity-modulated radiation therapy on sciatic nerve injury caused by echinococcosis

https://doi.org/10.4103/1673-5374.293153

Received: May 7, 2019

Peer review started: July 10, 2019

Accepted: June 4, 2020

Published online: September 22, 2020

Wan-Long Xu[1, *], Dilimulati·Aikeremu[2], Jun-Gang Sun[2], Yan-Jun Zhang[2], Jiang-Bo Xu[2], Wen-Zheng Zhou[2], Xi-Bin Zhao[2], Hao Wang[2], Hong Yuan[2]

Graphical Abstract *Intensity-modulated radiation therapy has the same therapeutic effect on echinococcosis as conventional radiotherapy, and can reduce apoptosis of the sciatic nerve around foci caused by radiotherapy*

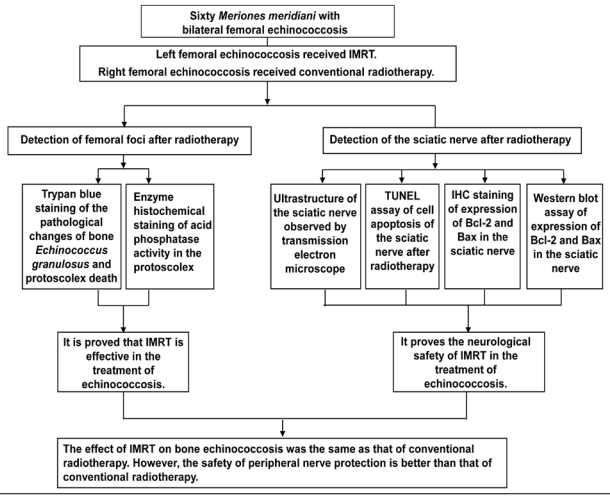

Abstract

Conventional radiotherapy has a good killing effect on femoral echinococcosis. However, the sciatic nerve around the lesion is irreversibly damaged owing to bystander effects. Although intensity-modulated radiation therapy shows great advantages for precise dose distribution into lesions, it is unknown whether intensity-modulated radiation therapy can perfectly protect the surrounding sciatic nerve on the basis of good killing of femoral echinococcosis foci. Therefore, this study comparatively analyzed differences between intensity-modulated radiation therapy and conventional radiotherapy on the basis of safety to peripheral nerves. Pure-breed *Meriones meridiani* with bilateral femoral echinococcosis were selected as the research object. Intensity-modulated radiation therapy was used to treat left femoral echinococcosis of *Meriones meridianus*, while conventional radiotherapy was used to treat right femoral echinococcosis of the same *Meriones meridianus*. The total radiation dose was 40 Gy. To understand whether intensity-modulated radiation therapy and conventional radiotherapy can kill femoral echinococcosis, trypan blue staining was used to detect pathological changes of bone *Echinococcus granulosus* and protoscolex death after radiotherapy. Additionally, enzyme histochemical staining was utilized to measure acid phosphatase activity in the protoscolex after radiotherapy. One week after radiotherapy, the overall structure of echinococcosis in bilateral femurs of *Meriones meridiani* treated by intensity-modulated radiation therapy disappeared. There was no significant difference in the mortality rate of protoscoleces of *Echinococcus granulosus* between the bilateral femurs of *Meriones meridiani*. Moreover, there was no significant difference in acid phosphatase activity in the protoscolex of *Echinococcus granulosus* between bilateral femurs. To understand the injury of sciatic nerve surrounding the foci of femoral echinococcosis caused by intensity-modulated radiation therapy and conventional radiotherapy, the ultrastructure of sciatic nerves after radiotherapy was observed by transmission electron microscopy. Additionally, apoptosis of neurons was examined using a terminal-deoxynucleotidyl transferase-mediated dUTP nick end labeling assay, and expression of Bcl-2 and Bax in sciatic nerve tissue was detected by immunohistochemical staining and western blot assay. Our results showed that most neurons in the left sciatic nerve of *Meriones meridiani* with echinococcosis treated by intensity-modulated radiation therapy had reversible injury, and there was no obvious apoptosis. Compared with conventional radiotherapy, the number of apoptotic cells and Bax expression in sciatic nerve treated by intensity-modulated radiation therapy were significantly decreased, while Bcl-2 expression was significantly increased. Our findings suggest that intensity-modulated radiation therapy has the same therapeutic effect on echinococcosis as conventional radiotherapy, and can reduce apoptosis of the sciatic nerve around foci caused by radiotherapy. Experiments were approved by the Animal Ethics Committee of People's Hospital of Xinjiang Uygur Autonomous Region, China (Approval No. 20130301A41) on March 1, 2013.

Key Words: apoptosis; factor; model; neuron; peripheral nerve; plasticity; protein; recovery; regeneration; repair

Chinese Library Classification No. R459.9; R453; R364

[1]Department of Orthopedics, Qilu Hospital of Shandong University, Jinan, Shandong Province, China; [2]Department of Orthopedics, People's Hospital of Xinjiang Uygur Autonomous Region, Urumqi, Xinjiang Uygur Autonomous Region, China

***Correspondence to:** Wan-Long Xu, MD, PhD, xuwanlong20082008@163.com.

https://orcid.org/0000-0002-5269-8987 (Wan-Long Xu)

Funding: *This work was supported by the China Postdoctoral Science Foundation, No. 2019M652397 (to WLX).*

How to cite this article: *Xu WL, Aikeremu D, Sun JG, Zhang YJ, Xu JB, Zhou WZ, Zhao XB, Wang H, Yuan H (2021) Effect of intensity-modulated radiation therapy on sciatic nerve injury caused by echinococcosis. Neural Regen Res 16(3):580-586.*

Introduction

Defects in surgical treatment to treat echinococcosis, such as the leakage of cyst fluid and hydatid cysts, can cause anaphylactic shock or even death. Recurrence rates of secondary infection of echinococcosis caused by leakage and residue of the protoscolex after operation, as well as various serious complications such as residual cavity infection and effusion, are as high as 25% (Chen et al., 2017a, b). Disadvantages of drug treatment include low drug concentration in the lesion site, unstable effect, long treatment cycle, problems with adherence, and low clinical efficiency and cure rates. Indeed, the cure rates of liver hydatid and pulmonary hydatid are only approximately 30%, and treatment of bone hydatid is mostly ineffective (Monge et al., 2017). Application of conventional radiotherapy for the treatment of bone echinococcosis has achieved good results in killing echinococcosis, and is expected to be the best choice in the clinic. However, irreversible radiation damage of important nerves around the lesion is often caused during radiotherapy and the disability rate is high, which hinders use of radiotherapy for bone echinococcosis (Xu et al., 2014). Compared with conventional radiotherapy, intensity-modulated radiation therapy (IMRT) is an advanced and high-precision radiotherapy that makes dose distribution more suitable for the target area of the focus, increases the dose of the focus, reduces the radiation dose of surrounding normal tissues and organs, improves the local control rate of the focus, and reduces the incidence of radiation injury of surrounding organs. However, it is unknown whether IMRT can both ensure good therapeutic effect and perfectly protect the surrounding sciatic nerve. To investigate the neurobiological safety of IMRT on echinococcosis of *Meriones meridiani*, this study observed the killing effect of IMRT on secondary echinococcosis and injury to sciatic nerve using conventional radiotherapy as a control.

Materials and Methods

Animals

Sixty adult male *Meriones meridiani* (aged 2–3 months and weighing 30.0 ± 6.5 g) were provided by the Institute of Experimental Animals of General Hospital of Chinese People's Armed Police Force, China (License No. SYXK (Jing) 2010-0025). X-ray and computed tomography (CT) examination of *Meriones meridiani* with echinococcosis revealed successful inoculation of echinococcosis in the femur. *Meriones meridiani* were housed in individual cages, provided complete feed and clean water, and maintained in a hygienic feeding environment at 20–23°C and humidity of 40–60%. Experiments were approved by the Animal Ethics Committee of People's Hospital of Xinjiang Uygur Autonomous Region, China (Approval No. 20130301A41) on March 1, 2013.

Group assignment and radiotherapy intervention

In all *Meriones meridiani* with bilateral femoral echinococcosis, left femoral hydatid lesions were treated with IMRT as the IMRT group, and right femoral hydatid lesions were treated with conventional radiotherapy as the conventional radiotherapy group.

First, the bilateral femoral echinococcosis area of 60 *Meriones meridiani* was determined as the target area of radiotherapy, and the surrounding blood vessels, tendons, nerves, and skin were deemed areas to be protected. After CT (Cleveland CT Factory, Cleveland, OH, USA) and computer-aided precise delineation of the radiation target area, and formulation of a radiotherapy plan, each *Meriones meridianus* was placed in the fixed mold or body membrane (Shandong Bainarui Analytical Instrument Technology Co., Ltd., Jining, Shandong Province, China) following inhalation anesthesia. According to the radiotherapy plan, IMRT (Xu et al., 2015) was performed within 14 days (rest on Saturdays and Sundays). Each radiotherapy dose of 4 Gy was administered during ten radiotherapy sessions; that is, the total dose was 40 Gy and the dose rate was 300 cGy/min.

Specimen collection and processing

One week after radiotherapy, *Meriones meridianus* with echinococcosis treated by IMRT were treated with inhalation anesthesia, and then sacrificed by air embolism. Under the microscope, cysts of *Echinococcus granulosus* in bilateral femoral bone marrow cavities were taken out. Part of the cyst fluid of *Echinococcus granulosus* was extracted for decompression. The remaining protoscoleces of *Echinococcus granulosus* were sucked out together with the cyst fluid, and the mixed suspension was divided into sterile polyethylene test tubes. Upper and lower edges of the sciatic nerve were determined according to the corresponding position of upper and lower edges of the focus of bone echinococcosis. After removal of the sciatic nerve, upper and lower edges were trimmed by 2 mm on each end to ensure that the sciatic nerve was located in the radiotherapy segment area. After removal from bilateral radiotherapy segments, sciatic nerves were fixed with 10% formaldehyde and 2.5% glutaraldehyde and stored in liquid nitrogen. After paraffin embedding, 4-μm sections were prepared and subjected to hematoxylin-eosin staining. Histological changes of the sciatic nerve were observed under an optical microscope (Leica, Wetzlar, Germany).

Trypan blue staining of pathological changes of bone *Echinococcus granulosus* and protoscolex death

One week after radiotherapy, suspensions of *Echinococcus granulosus* in sterile polyethylene tubes were stained with 1% trypan blue staining solution (Santa Cruz Biotechnology, Santa Cruz, CA, USA) for approximately 2 minutes and then smeared. The necrosis rate of protoscolex was observed and calculated under an inverted microscope (Leica). To judge the necrosis rate, trypan blue was used to stain structures of the dead protoscolex, as living protoscolex (with intact structure) cannot be stained with trypan blue. The necrosis rate (%) was equal to: (number of trypan blue stained protoscolex/number of all protoscoleces) × 100.

Enzyme histochemical staining of acid phosphatase activity in the protoscolex

Suspensions of the protoscolex of *Echinococcus granulosus* in sterile polyethylene test tubes were dried with a drying device and stained using the Gomori method. Glass slides with protoscoleces attached were dried with an electric blower. The incubation solution was added at room temperature (approximately 25°C) for 100 minutes until the color of slices was no longer deepened. Next, samples were washed with distilled water, followed by 1% glacial acetic acid for 1 minute, running water for 1 minute, 1% ammonium sulfide for 1 minute, and running water for 1 minute. Following staining with Nuclear Fast Red for 5 minutes, samples were observed under a microscope (Leica). Using a BT-2000 color pathological image analysis system (Hubei Botai Electronic Technology Co., Ltd., Wuhan, Hubei Province, China), ten visual fields were randomly selected from each image to measure average optical density.

Ultrastructure of the sciatic nerve observed by transmission electron microscope

One week after radiotherapy, specimens were washed with buffer solution and fixed with 2.5% glutaraldehyde for 2 hours, followed by 1% osmic acid for 2 hours, and then washed with phosphate-buffered saline (PBS). Specimens were dehydrated with increasing concentrations of ethanol and acetone, and then embedded, dried, incubated at 37°C overnight, and sliced into 50 nm-thick sections. Sections were observed and photographed with a transmission electron microscope (Hitachi, Hokkaido, Japan).

TUNEL assay of cell apoptosis of the sciatic nerve after radiotherapy

One week after radiotherapy, paraffin sections of the sciatic nerve were immersed in medical xylene solution for 4–5 minutes and then washed twice with a 1-minute interval. Sections were rehydrated in a gradient ethanol solution and then incubated with protease solution at 37°C for 20–30 minutes, followed by cell permeant solution for 6 minutes, and washed twice with PBS. After the slides were fully dried, 50 μL of TUNEL reaction mixture (Boehringer Mannheim, Berlin, Germany) were added and incubated at 37°C for 1 hour, followed by three washes with PBS. After the slides were fully dried, peroxidase (Boehringer Mannheim) was added and incubated at 37°C for 30 minutes, followed by three washes with PBS. Samples were incubated with 100 μL of diaminobenzidine solution at 15–25°C for 10 minutes, rinsed three times with PBS, and stained with hematoxylin. Afterwards, samples were visualized with diaminobenzidine (Boehringer Mannheim), dehydrated through a graded alcohol series, permeabilized with xylene, and mounted with neutral resin. Using a BT-2000 color pathological image analysis system, ten 20-fold visual fields with the densest apoptotic cells were selected in each slice to calculate the cell apoptotic index. The apoptotic index (%) was calculated as: average absorbance of positive cells × percentage of positive cells (in all cells in the visual field).

Immunohistochemical staining of Bcl-2 and Bax expression in the sciatic nerve

Using a streptavidin-biotin complex method, paraffin sections were dewaxed and hydrated. In accordance with kit instructions, sections were incubated with a primary antibody rabbit anti-canine Bcl-2 or Bax monoclonal antibody (1:100; Santa Cruz Biotechnology) at 4°C for 2 hours, followed by a secondary antibody rabbit anti-canine monoclonal antibody (1:100; Santa Cruz Biotechnology) at 37°C for 1 hour. Using BT-2000 color pathological image analysis system, ten visual fields were randomly selected from two areas in each section. The positively stained area was measured automatically, and the percentage of positively stained area in the visual field was calculated.

Western blot assay of Bcl-2 and Bax expression in the sciatic nerve

Cells were lysed with RIPA buffer (Santa Cruz Biotechnology) to extract total protein, which was quantified by bicinchoninic acid assay. Samples were then transferred onto polyvinylidene fluoride membranes, which were blocked with skimmed milk [Bright Food (Group) Co., Ltd., Shanghai, China], incubated with a primary rabbit anti-mouse monoclonal Bcl-2 or Bax antibody (β-actin, 1:2000; Bcl-2 and Bax, 1:200; Santa Cruz Biotechnology) at room temperature overnight. After washing, membranes were incubated with a secondary antibody rat anti-rabbit IgG (1:200; Santa Cruz Biotechnology) at room temperature. After washing, bands were visualized using an Odyssey Infrared Fluorescent Scan Imaging System (Li-Cor, Lincoln, NE, USA). Glyceraldehyde-3-phosphate dehydrogenase (GAPDH) was used as an internal control. Membranes were incubated with a chemiluminescence substrate and then exposed and developed by X-ray film. Images were scanned and saved as computer files. ImageJ 1.63 software (National Institutes of Health, Bethesda, MD, USA) was used to digitize the gray value of each specific band on the image. Gray values of Bcl-2 and Bax proteins were divided by the gray value of internal control GAPDH to correct for differences in total protein. The obtained results represent the relative content of Bcl-2 and Bax proteins, which are involved in apoptosis of bone *Echinococcus granulosus*.

Statistical analysis

Data were statistically processed by SPSS 19.0 software (IBM, Armonk, NY, USA) and expressed as the mean ± SD. Paired *t* test was used to compare means between the two groups, and paired χ^2 test was used for to compare mortality rates between the two groups. A value of $P < 0.05$ was considered statistically significant.

Results

Quantitative analysis of experimental animals

A total of 60 *Meriones meridiani* were included in the experiment. Left femoral echinococcosis of *Meriones meridianus* was treated with 40 Gy of IMRT, while right femoral echinococcosis of the same *Meriones meridianus* was treated with 40 Gy of conventional radiotherapy. Using this self-control model, 60 *Meriones meridiani* were involved in the result analysis.

Morphology of radiation area in *Meriones meridianus* after radiotherapy

None of the 60 *Meriones meridiani* died, but four animals exhibited decreased food intake after radiotherapy. There was no hair loss, skin necrosis, or ulceration on the IMRT side of any animal. Sciatic nerve paralysis occurred in all 60 *Meriones meridiani* on the conventional radiotherapy side with different degrees of hair loss, and skin ulcers appeared in three animals; neurological symptoms and skin ulcers did not recover before animals were sacrificed.

Pathological changes of bone *Echinococcus granulosus* and dead protoscolex after radiotherapy

Damaged protoscolex had a reduced ability to reject trypan blue staining, and the protoscoleces were stained blue. Trypan blue staining showed that the overall protoscolex structure in the bilateral femoral bone disease area disappeared: the outline lost its full state and collapsed, the color of the protoscolex was turbid, and dark blue was present (**Figure 1**). Mortality rates of protoscoleces on left femoral foci were not significantly different between IMRT group (57.71% ± 17.98%) and conventional radiotherapy groups (56.85% ± 16.60%) ($P > 0.05$).

Acid phosphatase activity in protoscoleces of *Echinococcus granulosus* in femurs following radiotherapy

Acid phosphatase is involved in the absorption and transportation of sugar and other substances, as well as the metabolism of carbohydrates. Decreased acid phosphatase activity affects the uptake of glucose and other nutrients by parasites. In addition, acid phosphatase is a marker enzyme of lysosomes that reflects their functional state. When cells are damaged by radiation, they undergo degeneration and necrosis, and the number and activity of lysosomes increase. Under these conditions, acid phosphatase activity increases, which may lead to increased cell membrane permeability and the promotion of organelle decomposition.

When the lysosomal membrane is stable and complete, substrates cannot easily penetrate the membrane and acid phosphatase activity is weak or inactive. After fixation (and under appropriate pH conditions), the membrane itself becomes unstable and gradually changes its permeability. At this point, the substrate can penetrate and enzyme activity is revealed. Acid phosphatase was strongly expressed in bone *Echinococcus granulosus* in left femurs treated with IMRT, as indicated by brown and evenly distributed staining, and locally agglomerated in the intensively stained area. Succinate dehydrogenase was also highly expressed in protoscoleces of *Echinococcus granulosus* in right femurs that received conventional radiotherapy. Average optical density of acid phosphatase products was 0.8901 ± 0.0977 for left femoral foci receiving IMRT, and 0.8992 ± 0.0960 for right femoral foci receiving conventional radiotherapy; there was no significant difference between the two groups ($P > 0.05$; **Figure 2**).

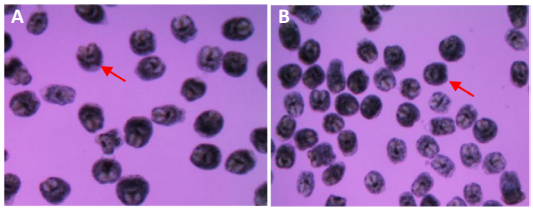

Figure 1 | Pathological changes of the protoscolex of bone *Echinococcus granulosus* 1 week after radiotherapy (trypan blue staining).
(A) Pathological changes of the protoscolex of bone *Echinococcus granulosus* after IMRT: The protoscolex of *Echinococcus granulosus* showed dark blue deposition and cell necrosis (arrow). (B) Pathological changes of the protoscolex of bone *Echinococcus granulosus* after conventional radiotherapy: The protoscolex of *Echinococcus granulosus* exhibited dark blue depositions and cell necrosis (arrow). Original magnification, 10× (optical microscope). IMRT: Intensity-modulated radiation therapy.

Morphology of sciatic nerve neurons following radiotherapy

Hematoxylin-eosin staining showed that for *Meriones meridiani* with echinococcosis treated by IMRT, most neurons in the left sciatic nerve exhibited normal morphology and had reversible injury, and apoptotic cells were rare. A small number of neurons lost polarity and became triangular, and there were lightly stained Nissl bodies, nuclear edema, and deviation. In contrast, *Meriones meridiani* treated with conventional radiotherapy commonly exhibited apoptotic cells in the right sciatic nerve. Moreover, a large number of neurons lost their polar appearance, and Nissl bodies disintegrated and disappeared. In addition, pyknosis, karyorrhexis, and karyolysis were observed. Some cells exhibited a fuzzy structure, dissolved nuclei, and disintegrated nuclear and cell membranes (**Figure 3**).

Morphology of neurons in the sciatic nerve

Under the transmission electron microscope, most neurons in the left sciatic nerves of *Meriones meridiani* with echinococcosis (IMRT group) presented normal morphology, with intact cell membranes, normal organelles, and basically normal nuclei. A few neurons exhibited slightly swollen mitochondria. In contrast, neurons of the right sciatic nerves of *Meriones meridiani* with echinococcosis (conventional radiotherapy group) exhibited loose cytoplasm, swollen mitochondria, broken cristae, and even cavitation. Moreover, the rough endoplasmic reticulum of these neurons was expanded and degranulated, the space between nuclear membranes was widened, and pyknosis and nuclear disintegration were visible. Chromatin was condensed and agglomerated in the nuclear membrane, which was surrounded by crescent-shaped or ring-shaped bodies; in addition, apoptotic bodies could be seen (**Figure 4**).

Cell apoptosis in the sciatic nerve

In the IMRT group, no apoptotic neurons were found in the left sciatic nerves of *Meriones meridiani* with echinococcosis. In the conventional radiotherapy group, obvious cell apoptosis was observed in the right sciatic nerves of *Meriones meridiani* with echinococcosis (**Figure 5**). Moreover, the apoptotic index was significantly lower in the left sciatic nerve (IMRT group, 2.36 ± 0.42%) than the right sciatic nerve (conventional radiotherapy group, 86.77 ± 23.12%; $P < 0.05$).

Immunoreactivity of Bcl-2 and Bax in the sciatic nerve

Immunohistochemical staining showed that Bcl-2 protein-immunoreactive cells (brown, fine, and granular appearance) were mainly distributed in the cytoplasm, processes, and nuclear membrane of neurons in both groups; nuclei were not stained. Bax protein-immunoreactive cells were mainly distributed in the cell bodies and processes of neurons, and nuclei were lightly stained (**Figure 6**). Immunohistochemical staining results showed that the percentage of Bcl-2-immunoreactive area in the sciatic nerve was higher in the IMRT group compared with the conventional radiotherapy group ($P < 0.05$). Moreover, the percentage of immunoreactive area of the pro-apoptotic protein Bax was lower in the IMRT group compared with the conventional radiotherapy group ($P < 0.05$; **Table 1**).

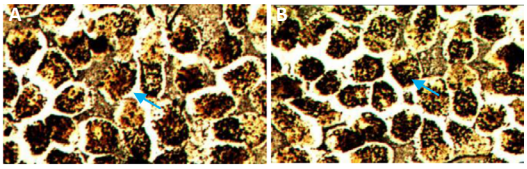

Figure 2 | Activity of acid phosphatase in protoscolex 1 week after radiotherapy (enzyme histochemical staining).
(A) Morphology of protoscolex after IMRT: Highly expressed acid phosphatase in protoscolex on the left femoral foci (arrow); (B) morphology of protoscolex after conventional radiotherapy: Highly expressed acid phosphatase in protoscolex on the right femoral foci (arrow). Original magnification, 40× (optical microscope). IMRT: Intensity-modulated radiation therapy.

Expression of apoptosis-related proteins Bcl-2 and Bax in the sciatic nerve

Western blot assay results showed that Bcl-2 protein expression was greatly increased and Bax protein expression was greatly inhibited in the IMRT group compared with the conventional radiotherapy group (**Table 1**).

Discussion

The results from this study showed no differences between IMRT and conventional radiotherapy with regard to the treatment of bone echinococcosis in *Meriones meridiani*. In this study, pure-breed *Meriones meridiani* with bilateral femoral echinococcosis were selected as the research object. IMRT was used to treat left femoral echinococcosis of *Meriones meridianus*, while conventional radiotherapy was used to treat right femoral echinococcosis of the same *Meriones meridianus*. The total radiation dose was 40 Gy. One week after radiotherapy, the overall structure of echinococcosis in bilateral femurs of *Meriones meridiani* treated with IMRT disappeared, as indicated by the presence of dark blue nuclei and cytoplasm stained with trypan. There was no significant difference in mortality rates of the protoscolex of *Echinococcus granulosus* between bilateral femurs of *Meriones meridiani*. Moreover, there was no significant difference in acid phosphatase activity in the protoscolex of *Echinococcus granulosus* between bilateral femurs. These findings indicate that IMRT and conventional radiotherapy could effectively kill femoral *Echinococcus granulosus*, consistent with numerous previous studies. Zhao et al. (2019) confirmed that radiotherapy is effective on echinococcosis in mice and proved that radiation can damage cell morphological structures and elicit cell death and apoptosis at a molecular level in hydatid cysts. Xu et al. (2014) used 40-Gy IMRT to treat echinococcosis in *Meriones meridiani* with radiotherapy for 2 weeks and found that IMRT can destroy the overall structure of the protoscolex of *Echinococcus granulosus*. The succinate dehydrogenase activity pathway was implicated in observed effects on the protoscolex of *Echinococcus granulosus* leading to death, suggesting that IMRT has a good therapeutic effect on secondary echinococcosis in *Meriones meridiani*. Mao et al. (2017) found that radiotherapy is a safe and effective method for the treatment of echinococcosis; the results of low-dose (30 Gy), moderate-dose (45 Gy), and high-dose (60 Gy) groups indicated a dose-effect relationship between the killing effect of echinococcosis foci and radiation dose. Yuan et al. (2016) demonstrated that *Echinococcus granulosus* cells were sensitive to radiotherapy, and irradiation at different doses of 10, 20, 40, and 80 Gy indicated that the recurrence rate of echinococcosis decreased with increasing radiation dose. A clinical study by Ulger et al. (2013) reported that a

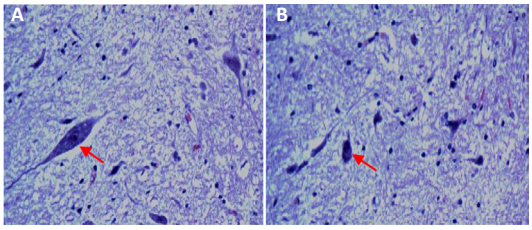

Figure 3 | Morphology of neurons in the sciatic nerve 1 week after radiotherapy (hematoxylin-eosin staining, optical microscope, 200×).
(A) Morphology of neurons in the left sciatic nerve of *Meriones meridianus* with echinococcosis was normal, with clearly visible axons on the left femoral foci in the IMRT group (arrow); (B) morphology of neurons in the right sciatic nerve of *Meriones meridianus* without echinococcosis; pyknosis and apoptosis appeared in the conventional radiotherapy group (arrow). IMRT: Intensity-modulated radiation therapy.

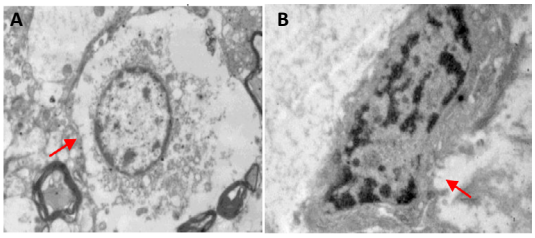

Figure 4 | Normal morphology of neurons in the sciatic nerve and slightly swollen mitochondria observed by electron microscopy.
(A, B) Neurons (arrows) of the left sciatic nerves of *Meriones meridiani* with echinococcosis in the IMRT group (A) and conventional radiotherapy group (B): Apoptotic bodies were visible. Original magnification, 8000× (transmission electron microscope). IMRT: Intensity-modulated radiation therapy.

Table 1 | Expression of Bcl-2 and Bax in the sciatic nerve after radiotherapy

	Group	Bcl-2	Bax
Immunoreactivity (percentage of positive area)	IMRT	27.96±7.54*	1.45±0.12*
	Conventional radiotherapy	2.11±0.25	37.44±11.27
Protein expression (gray value/GAPDH)	IMRT	11.22±2.77*	2.15±0.64*
	Conventional radiotherapy	3.71±0.65	17.19±3.32

*$P < 0.05$, *vs*. conventional radiotherapy group. Data are expressed as mean ± SD ($n = 60$; paired *t*-test). GAPDH: Glyceraldehyde-3-phosphate dehydrogenase; IMRT: intensity-modulated radiation therapy.

25-Gy dose of radiation therapy cured patients with sternal echinococcosis; notably, pain disappeared 1 year later in these patients, and no recurrence was found in multiple CT examinations. In contrast to previous studies (Xu et al., 2015, 2018; Van et al., 2016; Mihmanli et al., 2016.), this study compared the left and right sides of *Meriones meridiani*, which significantly improves experimental reliability and makes the results more convincing.

Our experimental results suggest that radiation can activate the metabolism of acid phosphatase in protoscoleces of *Echinococcus granulosus*, which alters its participation in the absorption and transport of sugars and other substances, as well as carbohydrate metabolism, thereby affecting intake of glucose and other nutrients by the parasite. Moreover, our experimental results showed that the overall structure of the protoscolex of bone echinococcosis disappeared. All these results occurred because of increased production of acid phosphatase (the marker enzyme of lysosomes) after radiotherapy, which reflected that the number and function of lysosomes increased in echinococcosis cells. Moreover, the functional state of lysosomes was significantly improved, leading to increased cell membrane permeability, promotion of organelle decomposition, and ultimately cell damage, degeneration, and necrosis. The results described above

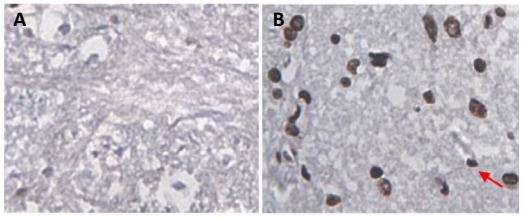

Figure 5 | TUNEL staining of apoptosis of cells in the sciatic nerve.
(A) No apoptotic cells in the left sciatic nerves of *Meriones meridiani* with echinococcosis in the IMRT group; (B) a large number of apoptotic cells (arrow) in the right sciatic nerves of *Meriones meridiani* with echinococcosis in the conventional radiotherapy group. Original magnification, 200× (optical microscope). TUNEL staining showed that the nuclei of normal cells in the sciatic nerve presented as light blue, whereas the nuclei of apoptotic cells were brown. IMRT: Intensity-modulated radiation therapy; TUNEL: terminal-deoxynucleotidyl transferase-mediated dUTP nick end labeling.

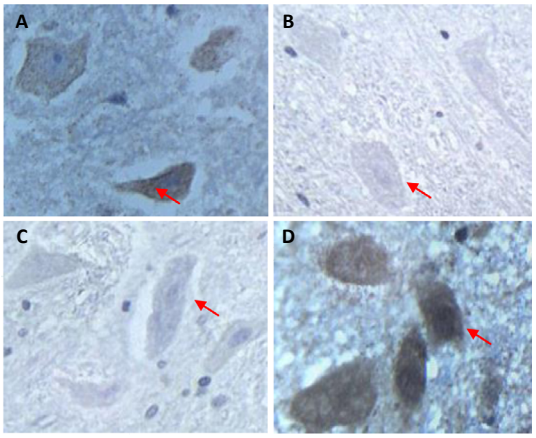

Figure 6 | Immunoreactivity of Bcl-2 and Bax in the sciatic nerve of both groups (immunohistochemical staining).
(A) A high number of Bcl-2-immunoreactive cells (arrow) in the IMRT group; (B) a low number of Bcl-2-immunoreactive cells (arrow) in the conventional radiotherapy group; (C) a low number of Bax-immunoreactive cells (arrow) in the IMRT group; (D) a high number of Bax-immunoreactive cells (arrow) in the conventional radiotherapy group. Original magnification, 400× (optical microscope). IMRT: Intensity-modulated radiation therapy.

indicate that IMRT could inhibit the growth of surviving protoscoleces *in vivo* and *in vitro*, eventually leading to parasite death possibly through the acid phosphatase pathway; this finding differs from the theory that radiation directly kills cells proposed by many scholars (Zhang et al., 2011; McManus et al., 2012; Xu et al., 2012; Neumayr, 2015; Chen et al., 2017a, b).

Experimental results regarding the biological safety of sciatic nerve indicated that 60 *Meriones meridiani* had symptoms of sciatic nerve paralysis on the that side received conventional radiotherapy but did not show any symptoms of sciatic nerve injury on the side that received IMRT. To clarify these results, the ultrastructure of sciatic nerves was observed after radiotherapy by transmission electron microscopy, apoptosis of neurons was examined using TUNEL assay, and Bcl-2 and Bax expression in sciatic nerve tissue was detected by immunohistochemical staining and western blot assay. Our results showed that most neurons in the left sciatic nerves of *Meriones meridiani* with echinococcosis treated by IMRT mainly had reversible injury, and there was no obvious apoptosis. Compared with conventional radiotherapy, numbers of apoptotic cells and expression of Bax in sciatic nerve treated with IMRT were significantly decreased, whereas Bcl-2 expression was significantly increased. These results suggest that compared with conventional radiotherapy, the number of apoptotic neurons in the sciatic nerve induced by IMRT was significantly reduced, and no obvious apoptosis was observed. In conclusion, these results indicate that radiation-induced neuropathy of the sciatic

nerve was produced by conventional radiotherapy, but IMRT can protect the sciatic nerve under a condition that normally kills *Echinococcus granulosus*. Thus, the biological safety of IMRT was better than that of conventional radiotherapy. With the rapid development of imaging and computer technology in recent years, radiotherapy has entered the era of precision radiotherapy, among which IMRT has become the most representative method (Kobayashi et al., 2013; Frenzel and Krüll et al., 2015; Akino et al., 2018; Li et al., 2018, 2020; Abu-Gheida et al., 2019; Tanaka et al., 2019; Morgan, 2020; Isono et al., 2020).

IMRT, a new radiotherapy technology developed in recent years, is characterized by the use of a three-dimensional treatment planning system to design coplanar or non-coplanar irregular fields for fractional irradiation. By adjusting the output dose rate of each point in the radiation field, the high-dose isodose line and plane are consistent with the target area in three-dimensional space. IMRT has the advantages of accurate and uniform dose irradiation on the target area, which significantly reduces the radiation dose of surrounding normal tissues. Under the premise of ensuring the local radiation dose and local control rate, the normal tissue complication probability is not increased (Lin et al., 2018; Chen et al., 2019; Cho et al., 2019; Lee et al., 2019; King et al., 2019; Mix et al., 2019; Ozkan, 2019; Zhang et al., 2019a, b; Dewan et al., 2020; Fabiano al., 2020; Murthy et al., 2020; Simões et al., 2020). However, experimental results vary from those published by Mohamed et al. (2019); namely, the tolerance dose of normal nerve tissue is 40–50 Gy/4–5 weeks, and radiation-induced neuropathy may be caused if this limit is exceeded (Doroslovački et al., 2018). Animal experiments conducted by Chargari et al. (2017) and Saager et al. (2018) showed that the occurrence of radiation-induced neuropathy is associated with many factors, such as the way and amount of radiation dose received, state of immune function, and duration of disease. Glicksman et al. (2020) proposed an important cause of disease when they showed that radiation-induced neuritis can occur when spinal cord neurons are irradiated more than 40–50 Gy1.8–2.0 Gy/time. Moreover, studies have verified that with increases of the total dose and amount of each division, or decreases of age, the risk of disease increases remarkably (Saager et al., 2020; Zeman et al., 2020). Akbas et al. (2019) reported that 10 years after radiotherapy for nasopharyngeal carcinoma, the incidence of nerve injury in the brain and spinal cord reached 18.6%. Bišof et al. (2018) reported that IMRT played a crucial role in reducing spinal nerve injury after radiotherapy for nasopharyngeal carcinoma. Our experimental results showed that sciatic nerves of the 40-Gy IMRT group did not show obvious radiation-induced neuritis. We believe these experimental results occurred because of the following reasons: (1) Because of its remarkable physical advantages, IMRT can control the direction of radiation by computer to concentrate accurate and high-dose rays on the lesion tissue, while rarely damaging the surrounding tissue; thus, sciatic nerve tissue adjacent to the femoral foci of echinococcosis was protected to the maximum extent. (2) The sensitivities of murine and human nerve tissue to radiation are different. (3) To ensure the safety of clinical treatments, the formulation of tolerated doses for human nerve tissue is conservative and relatively safe.

In conclusion, our comparison of neuronal morphology, apoptotic index, and pro-apoptotic and anti-apoptotic protein contents in sciatic nerve between two radiotherapy methods indicated that the biological safety of IMRT was significantly better than that of conventional radiotherapy. Indeed, IMRT had both a good therapeutic effect on echinococcosis and high neurobiological safety, thus providing an experimental basis for future studies. However, because this was only a preliminary animal study using a small number of experimental animals, and thus has a certain experimental bias, the results need verification through a large number of clinical studies to popularize and apply this result clinically.

Acknowledgments: *We thank Chun Zhang, animal breeder of Animal Laboratory of the First Affiliated Hospital of Xinjiang Medical University, and Yan-Jun Zhang, laboratory technician of People's Hospital of Xinjiang Uygur Autonomous Region, China, for their technical support.*
Author contributions: *Provision and integrity of the data, drafting of the manuscript, and fundraising: WLX; study concept and design, critical revision of the manuscript: HW; provision of technical, or material support, and study performance: Dilimulati·Aikeremu, JGS, YJZ, JBX, WZZ, XBZ, and HY. All authors approved the final version of the paper.*
Conflicts of interest: *The authors declare that there are no conflicts of interest associated with this manuscript.*
Financial support: *This work was supported by the China Postdoctoral Science Foundation, No. 2019M652397 (to WLX). The funding source had no role in study conception and design, data analysis or interpretation, paper writing or deciding to submit this paper for publication.*
Institutional review board statement: *The experiment was approved by the Animal Ethics Committee of the People's Hospital of Xinjiang Uygur Autonomous Region, China (approval No. 20130301A41) on March 1, 2013. The experimental procedure followed the United States National Institutes of Health Guide for the Care and Use of Laboratory Animals (NIH Publication No. 85-23, revised 1996).*
Copyright license agreement: *The Copyright License Agreement has been signed by all authors before publication.*
Data sharing statement: *Datasets analyzed during the current study are available from the corresponding author on reasonable request.*
Plagiarism check: *Checked twice by iThenticate.*
Peer review: *Externally peer reviewed.*

References

Abu-Gheida I, Reddy CA, Kotecha R, Weller MA, Shah C, Kupelian PA, Mian O, Ciezki JP, Stephans KL, Tendulkar RD (2019) Ten-year outcomes of moderately hypofractionated (70 Gy in 28 fractions) intensity modulated radiotherapy for localized prostate cancer. Int J Radiat Oncol Biol Phys 104:325-333.

Akbas U, Koksal C, Kesen ND, Ozkaya K, Bilge H, Altun M (2019) Nasopharyngeal carcinoma radiotherapy with hybrid technique. Med Dosim 44:251-257.

Akino Y, Mizuno H, Tanaka Y Isono M, Masai N, Yamamoto T (2018) Inter-institutional variability of small-field-dosimetry beams among HD120TM multileaf collimators: a multi-institutional analysis. Phys Med Biol 63:205018-205029.

Bišof V, Rakušić Z, Bibić J, Grego T, Soče M (2018) Comparison of intensity modulated radiotherapy with simultaneous integrated boost (IMRT-SIB) and a 3-dimensional conformal parotid gland-sparing radiotherapy (ConPas 3D-CRT) in treatment of nasopharyngeal carcinoma: a mono-institutional experience. Radiol Med 123:217-226.

Chargari C, Maroun P, Louvel G, Drouet M, Riccobono D, François S, Dhermain F, Cosset JM, Deutsch É (2017) Repair and time-dose factor: the example of spinal cordirradiation. Cancer Radiother 21:6-7.

Chen X, Duan X, Shao Y, Jiang J, Zheng S, Wen H (2017a) Control of human echinococcosis in Xinjiang, China, with 2,544 surgeries in a multihospital network. Am J Trop Med Hyg 97:658-665.

Chen X, Zhang R, Aji T, Shao Y, Chen Y, Wen H (2017b) Novel interventional management of hepatic hydatid cyst with nanosecond pulses on experimental mouse model. Sci Rep 7:4491-4499.

Chen X, Zhu X, Wang J, Liu J, Ji R (2019) NACT+IMRT versus NACT+IMRT+CCRT in locoregionally advanced NPC patients: a retrospective study. Onco Targets Ther 12:1553-1562.

Cho IJ, Chung WK, Lee JK, Lee MC, Paek J, Kim YH, Jeong JU, Yoon MS, Song JY, Nam TK, Ahn SJ, Lee DH, Yoon TM, Lim SC (2019) Intensity-modulated radiotherapy for stage I glottic cancer: a short-term outcomes compared with three-dimensional conformal radiotherapy. Radiat Oncol J 37:271-278.

Dewan A, Chufal KS, Tandon S, Ahmad I, Suresh T, Dewan A, Pahuja A (2020) A case report evaluating combined effect of intensity-modulated radiotherapy and deep inspiratory breath-hold for mediastinal lymphoma: a dosimetric analysis. Lung India 37:57-62.

Doroslovački P, Tamhankar MA, Liu GT, Shindler KS, Ying GS, Alonso-Basanta M (2018) Factors associated with occurrence of radiation-induced optic neuropathy at "safe" radiation dosage. Semin Ophthalmol 33:581-588.

Fabiano S, Balermpas P, Guckenberger M, Unkelbach J (2020) Combined proton-photon treatments- A new approach to proton therapy without a gantry. Radiother Oncol 145:81-87.

Frenzel T, Krüll A (2015) The use of IMRT in Germany. Strahlenther Onkol 191:821-826.

Glicksman RM, Tjong MC, Neves-Junior WFP, Spratt DE, Chua KLM, Mansouri A, Chua MLK, Berlin A, Winter JD, Dahele M, Slotman BJ, Bilsky M, Shultz DB, Maldaun M, Szerlip N, Lo SS, Yamada Y, Vera-Badillo FE, Marta GN, Moraes FY (2020) Stereotactic ablative radiotherapy for the management of spinal metastases: a review. JAMA Oncol doi: 10.1001/jamaoncol.2019.5351.

Isono M, Akino Y, Mizuno H, Tanaka Y, Masai N, Yamamoto T (2020) Inter-unit variability of multi-leaf collimator parameters for IMRT and VMAT treatment planning: a multi-institutional survey J Radiat Res doi: 10.1093/jrr/rrz082.

King M, Joseph S, Albert A, Thomas TV, Nittala MR, Woods WC, Vijayakumar S, Packianathan S (2019) Use of amifostine for cytoprotection during radiation therapy: a review. Oncology 17:1-20.

Kobayashi N, Nakayama H, Osaka Y, Tachibana S, Nogi S, Tajima Y, Okubo M, Mikami R, Kanesaka N, Sugahara S, Hoshino S, Tsuchida A, Tokuuye K (2013) Tumor response after low-dose preoperative radiotherapy combined with chemotherapy for squamous cell esophageal carcinoma. Anticancer Res 33:1157-1161.

Lee HC, Lee JH, Lee SW, Lee JH, Yu M, Jang HS, Kim SH (2019) Retrospective analysis of intensity-modulated radiotherapy and three-dimensional conformal radiotherapy of postoperative treatment for biliary tract cancer. Radiat Oncol J 37:279-285.

Li WZ, Liu GY, Lin LF, Lv SH, Qiang MY, Lv X, Wu YS, Liang H, Ke LR, Wang DL, Yu YH, Qiu WZ, Liu KY, Guo X, Li JP, Zou YJ, Xiang YQ, Xia WX (2020) MRI-detected residual retropharyngeal lymph node after intensity-modulated radiotherapy in nasopharyngeal carcinoma: Prognostic value and a nomogram for the pretherapy prediction of it. Radiother Oncol 145:101-108.

Li Y, Wang J, Tan L, Hui B, Ma X, Yan Y, Xue C, Shi X, Drokow EK, Ren J (2018) Dosimetric comparison between IMRT and VMAT in irradiation for peripheral and central lung cancer. Oncol Lett 15:3735-3745.

Lin CY, Shiau AC, Ji JH, Lee CJ, Wang TH, Hsu SH, Liang JA (2018) A simple method for determining dosimetric leaf gap with cross-field dose width for rounded leaf-end multileaf collimator systems. Radiat Oncol 13:222-229.

Mao R, Zhang WB, Qi HZ, Jiang T, Wu G, Lu PF, Abudula Ainiwaer, Shang G, Xu L, Hao J, Shou X, Li HT, Li J, Zhang SA, Bao YX, Wen H (2017) Efficacy of radiotherapy for the treatment of cystic echinococcosis in naturally infected sheep. Infect Dis Poverty 6:88-97.

McManus DP, Gray DJ, Zhang W, Yang Y (2012) Diagnosis, treatment, and management of echinococcosis. BMJ 344:e3866-3866.

Mihmanli M, Idiz UO, Kaya C, Demir U, Bostanci O, Omeroglu S, Bozkurt E (2016) Current status of diagnosis and treatment of hepatic echinococcosis. World J Hepatol 8:1169-1181.

Mix M, Tanny S, Nsouli T, Alden R, Chaudhari R, Kincaid R, Rosenbaum PF, Bogart JA, Aridgides P (2019) Outcomes following stereotactic body radiotherapy with intensity-modulated therapy versus three-dimensional conformal radiotherapy in early stage non-small cell lung cancer. Lung Cancer (Auckl) 10:151-159.

Mohamed AA, Mathis T, Bensadoun RJ, Thariat J (2019) Radiation induced optic neuropathy: does treatment modality influence the risk? Bull Cancer 106:1160-1176.

Monge MB, Chamorro TS, López VR (2017) Management of osseous cystic echinococcosis. Expert Rev Anti Infect Ther 15:1075-1082.

Morgan HE, Sher DJ (2020) Adaptive radiotherapy for head and neck cancer. Cancers Head Neck 5:1-16.

Murthy V, Maitre P, Bhatia J, Kannan S, Krishnatry R, Prakash G, Bakshi G, Pal M, Menon S, Mahantshetty U (2020) Late toxicity and quality of life with prostate only or whole pelvic radiation therapy in high risk prostate cancer (POP-RT): a randomised trial. Radiother Oncol 145:71-80.

Neumayr A (2015) Radiotherapy of osseous echinococcosis: where is the evidence? Int J Infect Dis 33:75-78.

Ozkan EE, Ozseven A, Cerkesli ZAK (2020) Evaluating the predictive value of quantec rectum tolerance dose suggestions on acute rectal toxicity in prostate carcinoma patients treated with IMRT. Rep Pract Oncol Radiother 25:50-54.

Saager M, Peschke P, Welzel T, Huang L, Brons S, Grün R, Scholz M, Debus J, Karger CP (2018) Late normal tissue response in the rat spinal cord after carbon ion irradiation. Radiat Oncol 13:5-14.

Saager M, Glowa C, Peschke P, Brons S, Grün R, Scholz M, Debus J, Karger CP (2020) Fractionated carbon ion irradiations of the rat spinal cord: comparison of the relative biological effectiveness with predictions of the local effect model. Radiat Oncol 15:6-16.

Simões R, Miles E, Yang H, Le Grange F, Bhat R, Forsyth S, Seddon B (2020) IMRiS phase II study of IMRT in limb sarcomas: results of the pre-trial qa facility questionnaire and workshop. Radiography (Lond) 26:71-75.

Tanaka Y, Mizuno H, Akino Y,Isono M, Masai N, Yamamoto T (2019) Do the representative beam data for TrueBeamTM linear accelerators represent average data? J Appl Clin Med Phys 20:51-62.

Ulger S, Barut H, Tunc M , Aydin E, Aydınkarahaliloğlu E, Gokcek A, Karaoğlanoğlu N (2013) Radiation therapy for resistant sternal hydatid disease. Strahlenther Onkol 189:508-509.

Van Cauteren D, Millon L, De Valk H, Grenouillet F (2016) Retrospective study of human cystic echinococcosis over the past decade in France, using a nationwide hospital medical information database. Parasitol Res 115:4261-4265.

Xu WL, Xilinbaoleri, Liu H, Wang RZ, Bai JP (2012) Spinal cord biological safety of image-guided radiation therapy versus conventional radiation therapy. Neural Regen Res 7:2755-2760.

Xu WL, Zhao XB ,Wang Q, Sun JG, Xu JB, Zhou WZ, Wang H ,Yan SG, Yuan H (2014) Three-dimensional conformal intensity-modulated radiation therapy of left femur foci does not damage the sciatic nerve. Neural Regen Res 9:1824-1829.

Xu WL, Tayerjiang, Zhao XB, Wang H, Wang Q, Yuan H (2015) Study of optimal scheme of spinal image-guided radiotherapy based on expression of caspase-3 in spinal cord neurons by orthogonal design. Genet Mol Res 14:3223-3233.

Xu WL, Xiang C , Wang H, Yuan H, Zhao XB, Xiao XY (2018) Effect of zoledronic acid therapy on postmenopausal osteoporosis between the Uighur and Han population in Xinjiang: an open-label, long-term safety and efficacy study. J Clin Pharm Ther 43:336-341.

Yuan Q, Li B, Jiang SP, Zhao Q, Duo J, Huang X (2017) Gamma-ray treatment of echinococcus protoscoleces prior toimplantation in mice reduces echinococcosis. BioMed Res Int 18:1-9.

Zeman RJ, Wen X, Moorthy CR, Etlinger JD (2020) Therapeutic target for external beam x-irradiation in experimental spinal cord injury. J Neurosurg Spine 3:1-8.

Zhang H, Chen Y, Hu Y, Yang P, Wang B, Zhang J, Sun J, Zeng Z (2019a) Image-guided intensity-modulated radiotherapy improves short-term survival for abdominal lymph node metastases from hepatocellular carcinoma. Ann Palliat Med 8:717-727.

Zhang N, Gu M, Wang J, Wu S (2019b) Comparison of nodal irradiation dose using radiotherapy for patients with thoracic esophageal cancer. Oncol Lett 19:1042-1050.

Zhang YC, Xie ZR, Ni YQ, Mao R, Qi HZ, Yang YG, Jiang T, Bao YX (2011) Curative effect of radiotherapy at various doses on subcutaneous alveolar echinococcosis in rats. Chin Med J 124:2845-2848.

Zhao YM, Gui WF, Zhang YS, Mo G, Li DY, Chong SG (2019) Inhibitory effect of ionizing radiation on echinococcus granulosus hydatid cyst. Diseases 7:1-10.

C-Editor: Zhao M; S-Editors: Wang J, Li CH; L-Editors: Deusen AV, Raye W, Qiu Y, Song LP; T-Editor: Jia Y